# THE OPTIMIZATION OF HIGH EFFICIENT PROPELLER

**Ivan Dofek**
Institute of Aerospace Engineering
Faculty of Mechanical Engineering
Brno University of Technology
Technická 2896/2
616 69 Brno
Czech Republic
dofek@fme.vutbr.cz

**Abstract.** The article deals with high efficiency propeller design procedure. A few methods for propeller performance design are described. Some of these methods are used for test case design and optimization. Aeroacoustics analyse of propeller is discussed.

**Keywords**. FWH, optimization, propeller, propeller blade, propeller noise, SOMA

## 1 Introduction

An ecological constrains, fuel prices and other factors cause any application of a new and progressive approaches in aircraft industry. One of the branches of application are propellers as part of propulsion system.

The objective of this paper is to present a research of the optimal design propeller procedure for small propeller aircraft and Mini UAV. The present research deals with propeller optimization constrained by noise and high efficiency. The research is divided into several main parts. The theoretical procedure for propeller design and analysis is the first main part of research. There are described propeller performance design procedures. The next part of research is focused on propeller optimization and application of some optimization techniques. The using of optimization algorithm SOMA is included in procedure. The optimization algorithm SOMA is briefly described and tested. The next and last part of research is focused on propeller noise analysis by application Ffowcs-Williams Hawkings equation. Practical application of theoretical propeller design procedure is applied on MINI UAV - VUT- 700 Specto. The research area of interest is shown on figure 1.

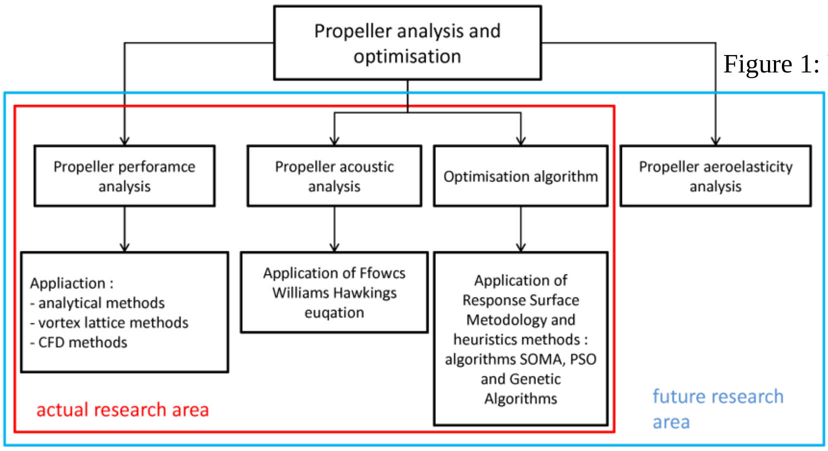


Figure 1: Flowchart of research interest

# 2 Propeller procedure design

## 2.1 A brief introduction to the used propeller performance procedures

There are a lot of approaches in literature which are focused on propeller design procedure, analysis of arbitrary design of propeller. These approaches differ mainly in accuracy of the gained distribution of the aerodynamics loads along the propeller blades and the blade section chord, the complexity of numerical solution and computing time. One of the approaches are analytical processes. They have good accuracy, low computing time and their complexity of numerical solution is not problematic. It is only possible to gain distribution of the aerodynamics loads along the propeller blades.
The most of applied theoretical design procedures for propeller performance design are based on work of Larrabee (1), Adkins (2) and Brož [03].The inverse design procedure with prescribed chord distribution is described in Hepperle [04]. The optimal distribution of circulation with minimal induced loses is main and common characteristics of these methods.
The next generation step in propeller design and analysis are vortex lattice methods Sullivan (5), Burger (06), Baskin (7), Dostál(8) and application of a potential flow solvers Carley (9).
Any application of CFD methods is the final generation step in the analysis, design and optimization of propellers. There are many cases of using commercial CFD solvers Dofek (10) or special CFD solvers for quick and accurate propeller performance analysis Pagano (11). Complexity analysis and solver options are the main advantages of using a CFD methods. There is possibility to simulate complex geometries of aircraft with a running propeller Steurmer (12).

## 2.2 Propeller design with minimum induced losses

The use of propeller performance with minimum induced losses is demonstrated. In the paper the theory is applied on theoretical test case flight conditions. The propeller design procedure is used in part of this paper which concern with noise propeller analysis for loading blade distribution. The conditions for minimum induced losses is called by Betz (16). The propeller design procedure is based on application of momentum theory, circulation equation and momentum loss tip function. The procedure is programmed in Python language. The procedure is described in Adkins (2).

### 2.2.1 Main system equation of propeller design procedure

This propeller design procedure is used for theoretical test case of propeller for specified flight conditions. Because of this facts, this design propeller procedure is described slightly in more detail.

Prandtl momentum loss function

$$F = \frac{2}{\pi} \cdot \arccos\left(e^{-f}\right) \quad [01] \qquad f = \frac{B}{2} \cdot \frac{(1-\xi)}{\sin(\phi_{tip})} \quad [02]$$

Flow angle at the tip propeller blade, flow angle at the

$$\phi_{tip} = \arctan\left(\lambda \cdot \left(1 + \frac{\zeta}{2}\right)\right) \quad [03] \qquad \phi = \arctan\left(\frac{\lambda}{\xi} \cdot \left(1 + \frac{\zeta}{2}\right)\right) \quad [04]$$

Cirkulation function

$$G = F \cdot x \cdot \sin(\phi) \cdot \cos(\phi) \quad [05]$$

Derivation respect to $\xi$ for thrust

$$\frac{\partial I_1}{\partial \xi} = 4 \cdot \xi \cdot G \cdot (1 - \varepsilon \cdot \tan(\phi)) \quad [06]$$

$$\frac{\partial I_2}{\partial \xi} = \lambda \cdot \frac{\partial I_1}{\partial \xi} \frac{1}{2 \cdot \xi} \cdot (1 + \varepsilon / \tan(\phi)) \cdot \sin(\phi) \cdot \cos(\phi) \quad [07]$$

**Blade geometry equations**

Derivation respect to $\xi$ for power

$$\frac{\partial J_1}{\partial \xi} = 4 \cdot \xi \cdot G \cdot (1 + \varepsilon / \tan(\phi)) \quad [08]$$

$$\frac{\partial J_2}{\partial \xi} = \frac{1}{2} \cdot \frac{\partial J_1}{\partial \xi} \cdot (1 - \varepsilon \cdot \tan(\phi)) \cdot \cos^2 \phi \quad [09]$$

$$Wc = 4\pi\lambda GVR\zeta / (c_l B) \quad [10]$$

$$W = V \cdot (1 + a) / \sin(\phi) \quad [11]$$

$$a = \frac{\zeta}{2} \cdot \cos^2(\phi) \cdot (1 - \varepsilon \cdot \tan(\phi)) \quad [12]$$

**Constrain equations**

$$T_C = \frac{2 \cdot T}{\rho \cdot V^2 \cdot \pi \cdot R^2} \quad [13]$$

$$P_C = \frac{2 \cdot P}{\rho \cdot V^3 \cdot \pi \cdot R^2} = \frac{2 \cdot Q \cdot \Omega}{\rho \cdot V^3 \cdot \pi \cdot R^3} \quad [14]$$

$$I_1 = \int_{\xi_{hub}}^{1} \left( \frac{\partial I_1}{\partial \xi} \right) \cdot d\xi \quad [14]$$

$$I_2 = \int_{\xi_{hub}}^{1} \left( \frac{\partial I_2}{\partial \xi} \right) \cdot d\xi \quad [15]$$

$$J_1 = \int_{\xi_{hub}}^{1} \left( \frac{\partial J_1}{\partial \xi} \right) \cdot d\xi \quad [16]$$

$$J_2 = \int_{\xi_{hub}}^{1} \left( \frac{\partial J_2}{\partial \xi} \right) \cdot d\xi \quad [17]$$

if the thrust is specified, the constrain equations are

$$\zeta = \frac{I_1}{2 \cdot I_2} - \sqrt{\left( \frac{I_1}{2 \cdot I_2} \right)^2 - \frac{T_c}{I_2}} \quad [18]$$

$$P_c = J_1 \cdot \zeta + J_2 \cdot \zeta^2 \quad [19]$$

if the power is specified, the constrain equations are

$$\zeta = -\frac{J_1}{2 \cdot J_2} - \sqrt{\left( \frac{I_1}{2 \cdot I_2} \right)^2 + \frac{P_c}{I_2}} \quad [20]$$

$$T_c = I_1 \cdot \zeta - I_2 \cdot \zeta^2 \quad [21]$$

### 2.2.2 Numerical scheme of propeller design procedure

Input data tip diameter R, number of blades B, air density ρ, flight velocity V, angular velocity of the propeller Ω, required thrust T or power consumption P and characteristics of used airfoils.
The procedure is taken from Adkins (2).
1. Selection of initial estimate of $\zeta$ ($\zeta = 0$ can be used at the start)
2. Determination of the values of F and $\phi$ for all blade stations using equations [01] to [04]
3. Computation of the product $Wc$
4. Determine $\varepsilon$ and $\alpha$ for airfoil section data, Cl
5. Determine $a$ and from equations [11], and W form equations [12].
6. Compute the chord from step 3, and the blade twist $\beta = \alpha + \phi$.
7. Determine the four derivates in $I$ and $J$ from Eq. XX and numerical integrate from these from $\xi = \xi_0$ to $\xi = 1$.
8. Determine $\zeta$ and $P_c$ from equations [18] and [19], or $\zeta$ and $T_c$ from equations [20] and [21].
9 If a new value of $\zeta$ is not sufficiently close to the old one (0.1%), start over at step 2 using new value of $\zeta$.
10. Determine propeller efficiency as $T_c / P_c$ and other features

### 2.2.3 Validation test case of propeller design procedure

The test case of the propeller design procedure is described in Adkins (2). The test case is computed for specific flight conditions and propeller geometry with NACA 44XX airfoil. The data are given in table 1. There is good agreement between paper test cases and programmed procedure. The difference between results is below 3%.

| input | unit | value |
|---|---|---|
| power | [kw] | 52000 |
| blades | [-] | 2 |
| Rtip | [m] | 0.8763 |
| rhub | [m] | 0.1524 |
| cl | [-] | 0.7 |
| speed | [km/h] | 177 |
| rpm | [1/min] | 2400 |
| output [XX] | | |
| thrust | [N] | 940 |
| ny | [-] | 0.87 |
| output [XX] | | |
| thrust | [N] | 930 |
| efficiency | [N] | 0.87 |

Table 1: Input a result propeller parameter, Adkins (1).

| r | c | φ | a | a' |
|---|---|---|---|---|
| [m] | [m] | [°] | [-] | [-] |
| 0.1524 | 0.104364 | 54.8118 | 0.0348 | 0.0633 |
| 0.27304 | 0.14036 | 38.3637 | 0.0644 | 0.0365 |
| 0.39371 | 0.130119 | 28.7661 | 0.0804 | 0.0219 |
| 0.51435 | 0.108783 | 22.7927 | 0.089 | 0.0142 |
| 0.63499 | 0.085222 | 18.7971 | 0.0938 | 0.0098 |
| 0.75566 | 0.058308 | 15.9619 | 0.0968 | 0.0072 |
| 0.8763 | 0.0000 | 13.3552 | 0.0000 | 0.0000 |

Table 2: Propeller geometry, Adkins (2).

| r | C | φ | A | a' |
|---|---|---|---|---|
| [m] | [m] | [°] | [-] | [-] |
| 0.1524 | 0.1062 | 54.9212 | 0.0352 | 0.0663 |
| 0.2731 | 0.1420 | 38.4769 | 0.0659 | 0.0386 |
| 0.3937 | 0.1311 | 28.8643 | 0.0828 | 0.0234 |
| 0.5144 | 0.1091 | 22.8758 | 0.0918 | 0.0153 |
| 0.6350 | 0.0853 | 18.8681 | 0.0953 | 0.0106 |
| 0.7557 | 0.0591 | 16.0234 | 0.0980 | 0.0078 |
| 0.8763 | 0.0000 | 13.5023 | 0.0000 | 0.0000 |

Table 3: Computed data, distribution along blade

### 2.3 Solution of isoperimetric problem and its application for optimal blade shape

This procedure is described in Brož (3). The task is to design the adjustable blade propeller. The shape of propeller blade is designed to have the best efficiency for one flight regime. The efficiency is defined by formula: $\eta = \frac{V_{oo} \cdot T}{N}$

For to find a solution of the isoperimetric problem, the task can be simply formulated as follows: find a closed flat curve of a given perimeter which encloses the largest area. The next formulation is used in application for optimization process : There are two given functions $F(x, y, y')$ and $\Phi(x, y, y')$ and task is : find a flat curve for which functional $G = \int_a^b \Phi(x, y, y')dx$ gets value of constant G and at the same time it leads to extreme of functional $I = \int_a^b F(x, y, y')dx$. The problem can be reduced in $H = \int_a^b \left[F(x, y, y') + \lambda \Phi(x, y, y')\right] dx$. The solution of functional corresponds with Euler differential equation $F'_y - \frac{d}{dx} F'_{y'} = 0$.

The function F can be thrust $\bar{T}(\bar{r}, \bar{\Gamma}, \bar{\Gamma}')$ or $\bar{N}(\bar{r}, \bar{\Gamma}, \bar{\Gamma}')$ in the same way like the function Φ can be thrust or power. These functions represent distribution of thrust coefficient or power coefficient along the propeller blade.

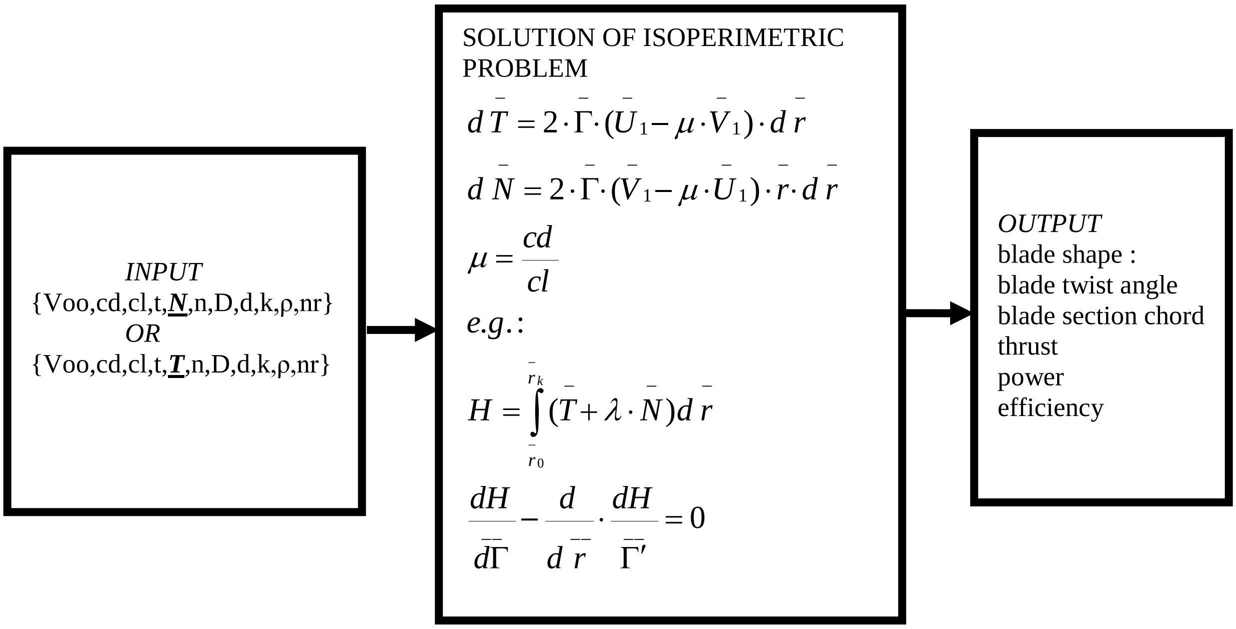


Figure 2: Flowchart of isoperimetric problem solution

### 2.4 Lifting line with circulation varying along its span

The procedure is described in Baskin (7). The propeller blade is divided into a few segments along radial direction. Induced velocities are computed on each radial station by application and solution of Biot - Savart Law. There is an assumption that the flow is at each radial station 2D. The solution procedure is very similar to solution of vortex lattice method. This procedure is programmed in Matlab and is used for test optimization case with evolutionary algorithm SOMA.

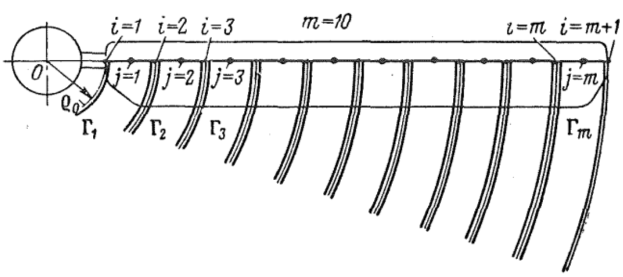


Figure 3: Propeller blade with lifting line.

The basics procedure equation :

$$v = \sum_{i=1}^{m} v_{ij} \cdot \Gamma_i \, (j = 1,2,..., m...number\_of\_radial\_segments) \text{ [22]}$$

The contribution at each radial control points is computed by integration equations 23 and 24 from 0 to infinity.

$$v_{ij} = \frac{1}{4 \cdot \pi} \sum_{i=1}^{k} \int_{0}^{\infty} \left[ P_{ij}(n, \vartheta) - P_{i+1j}(n, \vartheta) \right] d\vartheta \quad [23]$$

$$P_{ij}(n, \vartheta) = \frac{\overline{\rho}_i^{\,2} - \overline{\rho}_i \cdot r_j \cdot \cos(\delta_n - \vartheta)}{\left[ \overline{V}^2 \cdot \vartheta^2 + \overline{\rho}_i^{\,2} + r_j^{\,2} - 2 \cdot \overline{\rho}_i \cdot r_j \cdot \cos(\delta_n - \vartheta) \right]^{3/2}} \quad [24]$$

## 2.5 Brief description of vortex lattice method

The vortex lattice method is briefly described. There are a few types of vortex lattice method. One of the type vortex lattice method is described in Sullivan (5). There is propeller blade divided by helical horseshoe vortices in radial direction. In Dostál (8) and Baskin (7) is blade modelled by system of horseshoe vortices in radial and chord direction. There is possibility to include in solution the sweep of propeller blade.
The description of vortex lattice method is focused on theory and application described in Sullivan (9). The finding of induced velocity at the control point is a main principle solution vortex lattice methods. The induced velocity is due to bound and trailing vortices. There is applied boundary condition that the velocity (induced and free stream) normal to the surface must be zero.
That means :

$$\vec{v} \cdot \vec{n} = 0 \quad [25]$$

The velocity at control point j, *u,v,w* are induced velocities

$$\frac{v}{v_{oo}} = \left( \frac{u_j}{v_{oo}} - \frac{\omega \cdot r_j}{v_{oo}} \cdot \sin\theta_j \right) \cdot \vec{i} + \left( \frac{u_j}{v_{oo}} + \frac{\omega \cdot r_j}{v_{oo}} \cdot \cos\theta_j \right) \cdot \vec{j} + \left( 1 + \frac{w_j}{v_{oo}} \right) \cdot \vec{k} \quad [26]$$

Definition of horseshoe vortex at common control point j.

$$x = r \cdot \cos\theta, y = \sin\theta, z = \frac{v_\infty}{\omega \cdot R} \cdot \theta \quad [27]$$

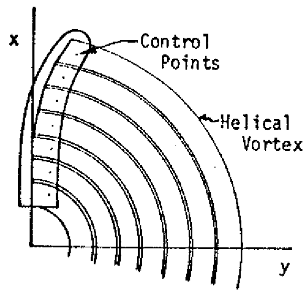


Figure 4: Propeller blade coordinate system, geometry with vortexes and control points.

### 2.6 CFD test cases of propeller

This part of research is focused on analysis of experimentally measured propeller. There are compared CFD simulations and propeller theory with experiment. There are presented two test cases of comparison  comparison of CFD simulation with experiment is presented.

The combined wind tunnel tests of force and wake survey NACA(23) were proceeded with three-blade propeller. There were seven propellers tested. They are labeled with numbers from 1 to 7. The propeller numbers from 1 to 6 have NACA 16 – series airfoil section along the propeller blade, united thickness and twist distribution and different blade section chord distribution. The forms of first six propellers are presented in figure 5. The propeller number 3 was selected as a CFD testing case. The CFD simulation is described in detail in Dofek (10). There is good agreement with experiment. It can be seen from presented graph.

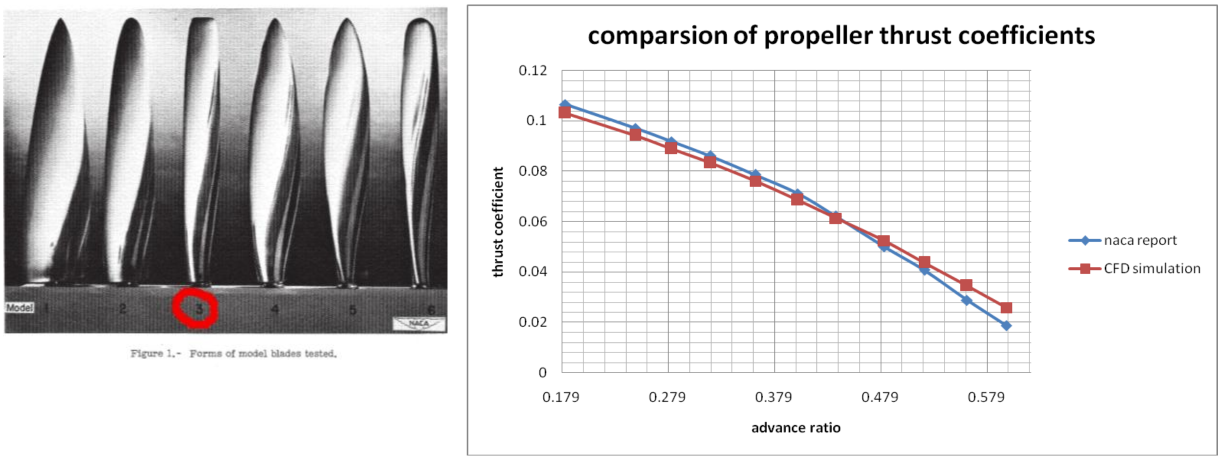


Figure 5: Propeller shape, comparison of the propeller thrust coefficient between experiment and CFD simulations.

The next CFD analysis was performed on a combined aeroacoustics wind tunnel experiment. There was made CFD model of squared propeller with Clark Y airfoil section. Only one test case is presented. The case is labeled AC - 1 in the report (21). test case conditions : rpm = 2100 rev/min, flow velocity 54.1 m/s, trust = 1549 N, power = 105.3 kW. test case results : trust 1511 N, power = 102.1 kW. The results differ about 3%. There is good agreement between CFD simulation and test data. On the figure 6. are presented propeller geometry and 3D model.

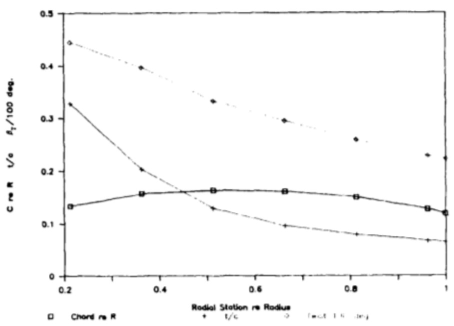

Radial Distributions of Blade-chord, -thickness
and -twist for the Square-tip Propeller (F9684-14)

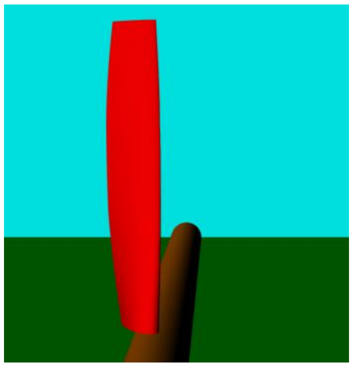

Figure 6: Test propeller case geometry ref. (21).

### 2.7 Test case of propeller design optimization with evolutionary algorithm SOMA

SOMA (Self-Organizating Migration Algorithm) is a stochastic optimization algorithm that works since 1999. The functioning of the algorithm is similar to PSO and Differential evolution Zelinka (15) and is based on operation with vectors. The name of SOMA describes its basic behaviour. The SOMA algorithm can be seen as a group of cooperating individuals that has a leader with a best properties. There are migrating individuals in the group who move to the leader of the group in N - dimensional space.

The application and testing of SOMA algorithm for global optimization problems is published in Zelinka (15), Zelinka (14) and Kurfürst (13). The test case of wing optimization is described in Zelinka (15). The algorithm is programmed in Python language and Matlab.

Main setup of parameters for SOMA algorithm :
step - this parameter describes the size of jump of each individuals
migrations - it is number of levels in which the population of individuals will be reorganized

#### 2.7.1 SOMA global optimization testing

The optimization algorithm SOMA is tested through application for number of global optimization test problems. There is presented one test problem with known position of global extreme. The main target of this application is finding a global extremes and tuning of SOMA control parameters. The test function is taken from Zelinka (15). The ability of SOMA algorithm for finding global extremes is briefly shown. For the presented test case is selected Ackleyho function.

The function has two global extrema
Global minimum : in E2...(-1.50236,-0.754865 or 1.50236,-0.754865), global extreme value = -4.5901
Test results : position( -1,50962010683666,-0,754865122328553), value = -4.590101634158668
Global minimum : in E10...(-1.51563,-1.1151,- 1.10972, ..., - 1.10972,-0.747245), global extreme value = -27.97345
Test results : position(1.5149, -1.1162, -1.1097, -1.1093, -1.1113, -1.1101, -1.1096, -1.1092, -1.1033, -0.7470), value = -27.9701

*Ackleyho function*

$$\sum_{i=1}^{D-1}\left(\frac{1}{e^5}\sqrt{\left(x_i^{\,2}+x_{i+1}^{\,2}\right)}+3\left(\cos\left(2x_i\right)+\sin\left(2x_{i+1}\right)\right)\right)$$

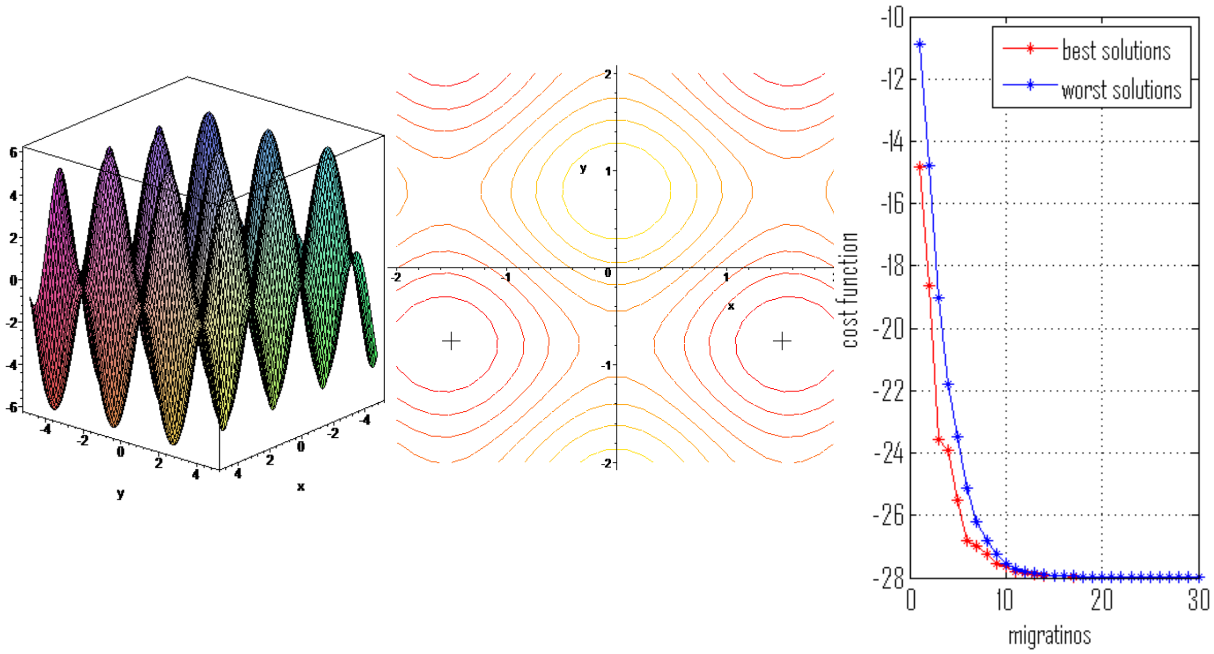


Figure 7: Test function, 3D function E2 graph, iso-contour with extremes, SOMA run

### 2.7.2 Optimization test case of optimal propeller design

Flight conditions:
flight speed 140 km/h, rpm 2000 ot/min, diameter 1.65 m, power 40000 kW, airfoil NACA 44XX

SOMA setup :
there was six variables, three variables for twist distribution and three variables for twist distribution.
step = 0.21/length of path = 2.1/prt = 0.1/ there was 16 migrations.

Propeller geometry was described by Bezier curve Linkeová (17). The target of optimization was the best efficiency for described power. There was used penalty function. The optimization was constrained by geometry and propeller absorbed power.
Results propeller with a minimum induced losses, for computation is used procedure Adkins (2)
flight speed 140 km/h, rpm 2000 rev/min, diameter 1.65 m, absorbed power 40000 kW, thrust 840 N, efficiency 0.82
optimized propeller, for computation is used procedure from chap. 2.4/Baskin (7)
flight speed 140 km/h, rpm 2000 rev/min, diameter 1.65 m, absorbed power 40000 kW, thrust 830 N, efficiency 0.81

Geometry distribution of minimum induced propeller and optimized propeller differs because of constrains. The optimized propeller satisfy the geometry and power constrains with the efficiency very close to the optimal minimum induced design propeller.

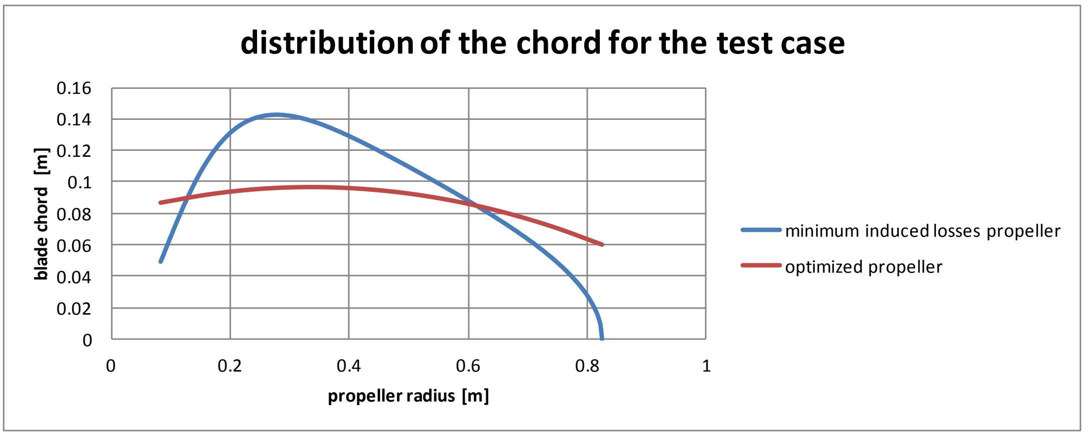


Figure 5: Distribution of the chord for the test case.

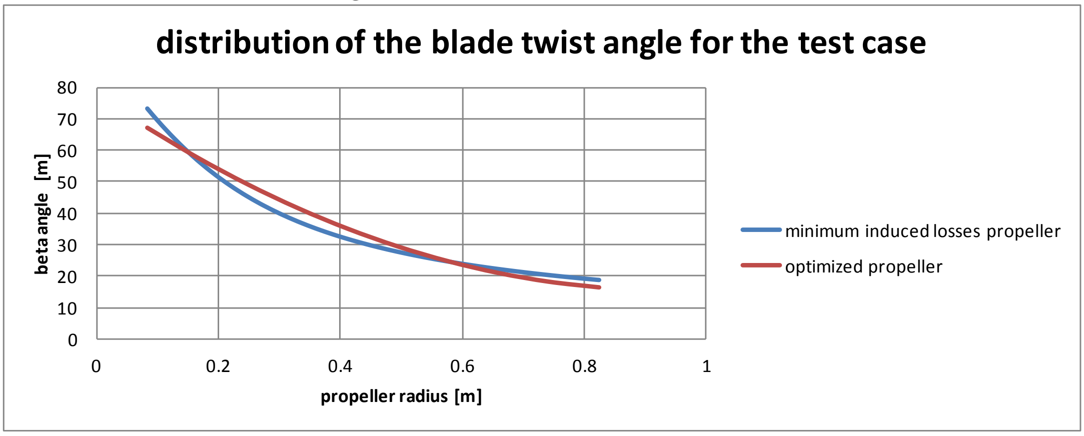


Figure 6: Distribution of the twist angle for the test case.

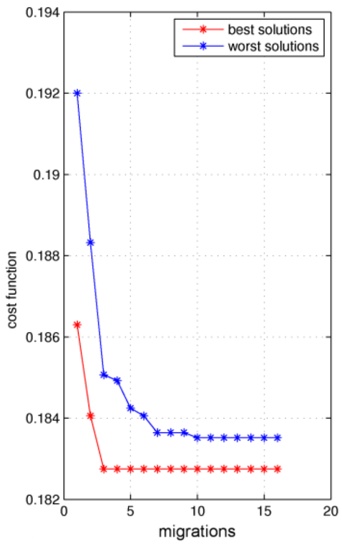


Figure 7: Distribution of the twist angle for the test case.

# 3 Propeller noise analysis

## 3.1 A brief propeller noise theory

$$\nabla^2 p - \frac{1}{c}\frac{\partial^2 p}{\partial x_i^2} = -\frac{\partial}{\partial t}\left\{\rho_0 \cdot v_n \cdot |\nabla f| \cdot \delta(f)\right\} + \frac{\partial}{\partial x_i}\left\{l_i \cdot |\nabla f| \cdot \delta(f)\right\} \quad [28]$$

There is linear form of Ffowcs Williams and Hawkings equation Farassat (19), Magliozi (20). The left side of equation represents linear wave operator. The right side contains noise source terms resulting from surface moving.
$\rho_0$ is ambient density, $c$ is ambient speed of sound, $v_n$ is the local velocity of the surface normal to itself, $\delta(f)$ is the Dirac delta function, $x_i$ is the observer position and $l_i$ is the ith component of the surface force.

## 3.2 The compact source formulas

For propeller noise analysis are derived in Succi (22) compact form of FWH equation. The compact source formula is obtained by application of Green's theorem. Afterwards this solution is discredited. In this application is propeller blade divided into small segments, compact noise source. Each segment has its own force vectors. The final noise is obtained by summing over all noise source contributions. This form of FWH equation is often used because of its simply programming simplicity and clarity. The basic division of the compact source formulas has two main part. Thickness and loading term. The thickness term represents the effect of the blades parting the air, thickness noise. The second term of this form represents the action of the blade forces on the air.

$$\Delta p(\bar{x},t) = \Delta p_{Thick}(\bar{x},t) + \Delta p_{Loading}(\bar{x},t) \quad [29]$$

$$4\pi p'(x,t) = \left[\sum_k \frac{1}{c}\frac{1}{|1-M_r|}\frac{\partial}{\partial \tau}\left(\frac{L_{ki}\vec{r}_i}{|1-M_r|}\right) + \frac{L_{ki}\vec{r}_i}{r^2|1-M_r|}\right]_{ret} + \sum_k \left[\frac{\rho_0 \psi_k}{|1-M_r|}\frac{\partial}{\partial \tau}\left(\left(\frac{1}{|1-M_r|}\right)\frac{\partial}{\partial \tau}\left(\frac{1}{r|1-M_r|}\right)\right)\right]_{ret}$$

[30]

**The algorithm function.**
The program structure for propeller noise analysis is in detail described in Farassat (18) and is programmed in the same way and description is very similar.
The following information are need for running of the program. Geometric data :
a) blade hub and tip radius, blade chord, thickness and twist distribution.
b) blade section distribution as function of radial coordinate
c) observer mode of motion, stationary or moving observer
Aerodynamics data:
blade loading or pressure distribution
Operating data:
propeller RPM and forward speed

The propeller blade is divided in to a few segments in accordance with application of compact formula. The number of elements (noise source) can be changed as necessary. The blade is replaced by number of points each with unique force vector and volume. The force vectors are obtained from propeller performance analysis. In this case, the loading data are obtained from blade element theory or lifting line theory.

After geometrical procedure, the second procedure the calculation of the noise source pressure signature. There is specified observer position at observer time t. In this application the observer position is stationary through the time. For the specified observer time, there is emission time for each noise source which is calculated by iterative scheme. In this case is used Brent method for solution of retarded time equation. At this retarded time, the contribution of a particular noise source is evaluated exactly according to equations [30]. The summation of all blade noise source yields to the pressure signature at observer time.

The program is programmed in Python language. There are used Python library Numpy, Scipy and Matplotlib. This libraries provide simply and effective output and input data exchange, numerical tools for solution of nonlinear equation of retarded time and output graph form. The equation are implemented in vector form.

After evaluation of signal there is used FFT algorithm which is implemented in Python. Afterwards there is possibility to use different filter e.g. A - weighted filter.

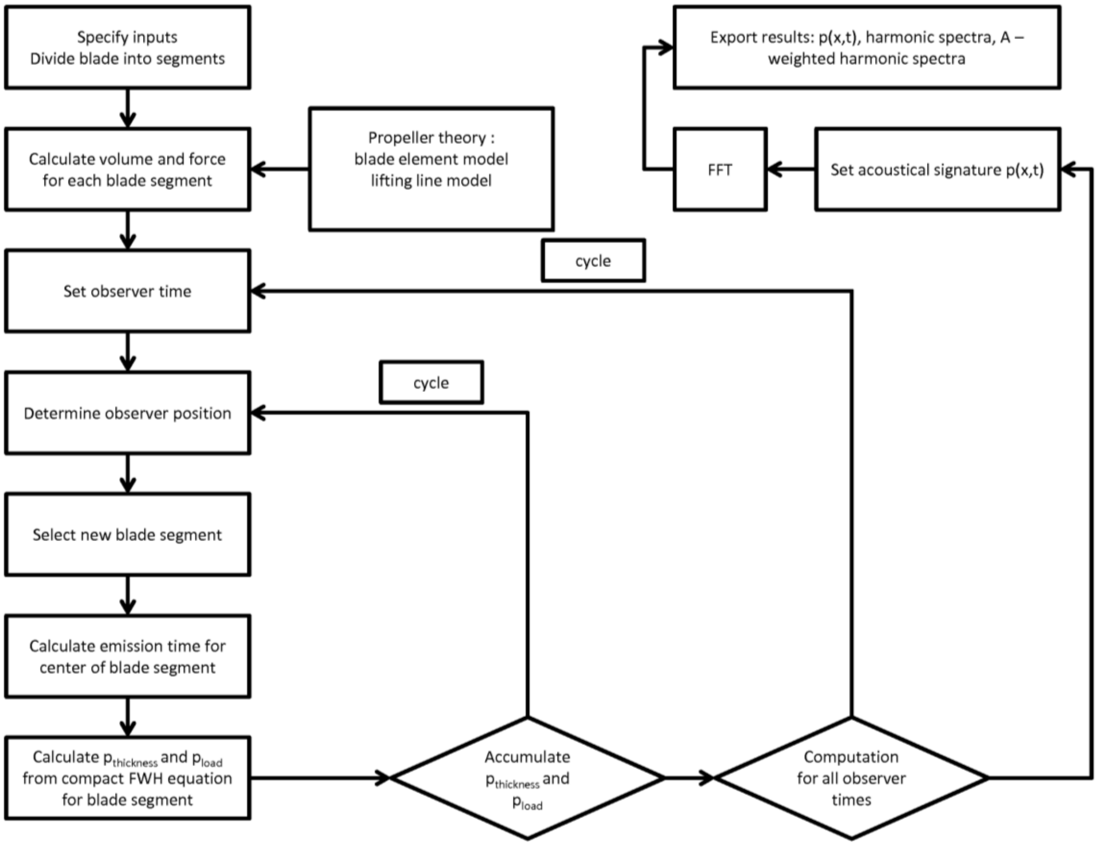


Figure 8: Application of FWH equations flowchart.

### 3.3 The basics test case of implemented FWH compact source formulas

There is performed basic test and validation of implementation FWH equation. The sense of this test is to check generated frequency spectra and compare it with experiment. For the test is selected the propeller noise test in wind tunnel (21). The test conditions and properties are described in (21). There is selected one test case of a wind tunnel test. The volume distribution is obtained from report (21) and loading distribution is obtained by application of propeller performance procedure according to test properties. There are information about propeller shape, loading and power. There is presented only one test case.

TEST BC-2
rpm 2100, flow velocity 54.1 m/s, power 105.3 kw, thrust 1549 N, Microphone No.9

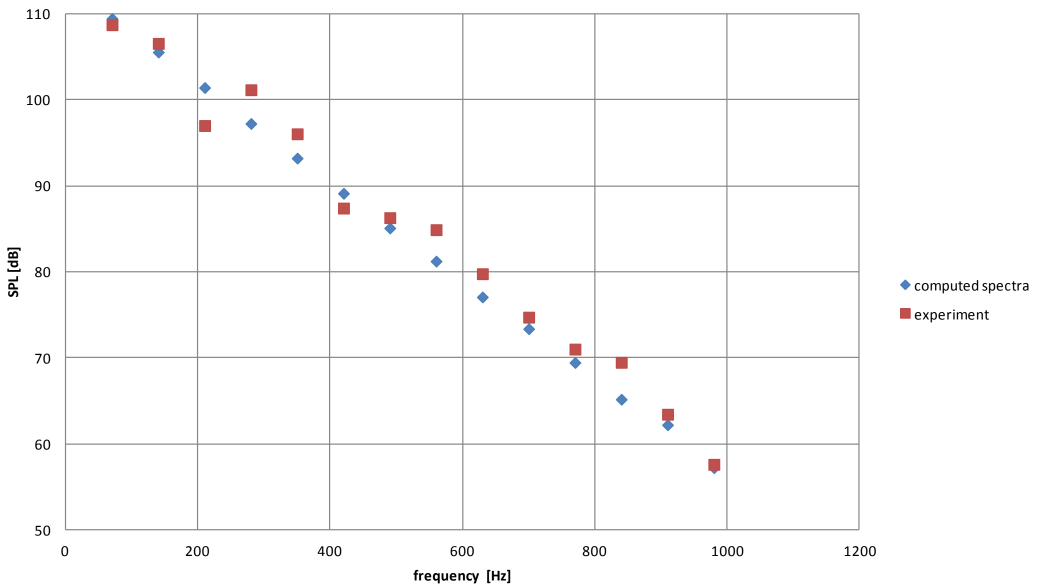


Figure 9: Comparison of computed and measured SPL frequency spectra, BC-2 .

There is good agreement between experimental and applied theory data. For the first and second harmonic number are differences very small.

# 4 Practical propeller performance procedure application

The part of the research is focused on practical application and production of propeller. This design process includes three parts: theoretical design of optimal blade shape, CAD design and production. All these three parts lead to composite adjustable propeller.
Solution of isoperimetric problem was used for propeller design performance and optimization.
The propeller was designed on specific flight conditions.

Input information

| | |
|---|---|
| free stream speed | Voo = 160 km/h |
| rotation speed | n = 6000 rpm |
| engine delivered power | N = 2.8 kW |

hub and tip diameter d = 0.05 m, D = 0.5 m
number of blades k = 2
flight level 0 m International Standard Atmosphere, ρ = 1.225 kg/m3
airfoil characteristics for NACA 44XX
drag-to-lift ratio is set at minimal value, about μ = 0.023
linear distribution of thickness along the propeller blade, hub diameter t = 30%, tip diameter t = 10%

Thrust T = 54.38 N, Power N = 2.79 kW, efficiency η = 86.5%.

The propeller was made and tested on MINI UAV VUT - 700 Specto. There have been several successful flights with this propeller.

Figure 10: The adjustable composite propeller and Mini UAV VUT - 700 Specto.

## 5 Conclusion

The paper presents a state of propeller design and optimization research. There are a few methods for propeller performance analysis discussed and some of these methods are used for the test optimization case.
The CFD simulations are briefly presented in the paper. This simulation was validated with wind tunnel test data and the results have good agreement. The data from this simulations will be used for detailed propeller aeroacoustics analysis.
The application of propeller noise analysis by using FWH equation is discussed and the implemented equation is applied on test case. There is need to detailed testing of the application of noise propeller analysis procedure for different conditions.
One of the propeller performance design procedure was applied to practical conditions and was successfully tested through a few flights.
The future work will be focused on multidisciplinary aeroacoustics and performance optimization by using different propeller performance analysis and optimization methods. The CFD methods will be used for propeller analysis and optimization. There is possible to obtain more detailed information about pressure distribution on propeller blade surface than using analytical approaches. The next stage in the future will be aeroelasticity analysis and optimization.

# References


(1)
Larrabee, E.E., "Practical Design of Minimum Induced Loss Propellers", SAE Preprint 790585, 1979
(2)
Charles N. Adkins and Robert H. Liebeck., Design of optimum propellers, Journal of Propulsion and Power, Vol. 10, No. 5 (1994), pp. 676-682.
(3)
Brož V., Aerodynamics Design of a Highly Efficient Propeller Blade, NASA TT F11,218
(4)
M. Hepperle, Inverse Aerodynamic Design Procedure for Propellers Having a Prescribed Chord Length Distribution, Journal of Aircraft, Volume 47, Number 6, November-December 2010.
(5)
Sullivan, J. P. The effect of blade sweep on propeller performance, Conference on Fluid and Plasmadynamics; 10th; June 27-29, 1977; Albuquerque, NM
(6)
Burger. Ch., Propeller Performance Analysis And Multidisciplinary Optimization Using A Genetic Algorithm, Dissertation, Auburn Alabama December 17, 2007
(7)
Baskin V.E., Theory of the lifting airscrew, NASA, February 1, 1976
(8)
Dostál J., Klímek P., Metoda aerodynamického výpočtu vrtule pomocí vírové mříže, část 1: Základní teorie, Letecký zpravodaj, No. 3/2008, str. 2 - 6
(9)
Orlando, C., Carley, M. and Marretta, R.M. A., 2009. Adaptive BEM for Low Noise Propeller Design. The Open Acoustics
(10)
Dofek I., The Propeller Design For Mini Uav Vut – 700 Specto, READ, International conference, June 2010, Warscava
(11)
Pagano A., Federico L., Barbarino M., GUida F., Aversano M.: Multi-objective Aeroacoustic Optimization of an Aircraft Propeller. In: 12th AIAA/ISSMO Multidisciplinary Analysis and Optimization Conference, Victoria, British Columbia Canada 62. Pierret S (1999) Turbomachinery, 2008
(12)
Stuermer A. W.: Unsteady CFD Simulations of Propeller Installation Effects, 42nd AIAA/ASME/SAE/ASEE Joint Propulsion Conference & Exhibit 9 - 12 July 2006, Sacramento, California
(13)
Kurfürst J., Optimization Algorithm SOMA Applied on The Vibration Generator, Ph.D. project.
(14)
Zelinka I., Comparison of an SOMA with Simulated Annealing and differential evolution for automated waveform tuning, Advances in Engineering Software 36 (2005) 645–653
(15)
Zelinka I., Evoluční výpočetní techniky - pricnipy a aplikace, Ben, Praha 2009, ISBN 978-80-7300-218-3
(16)
Betz A., with appendix by Prandtl L. Screw Propellers with Minimum Energy Loss, Gottingen Reports, 1919
(17)
Linkeová I.: NURBS křivky NeUnirofmní Racionální B-Spline křivky, ČVUT, Praha, 2007
(18)
Farassat F., A Review of Propeller Discrete Frequency Noise Prediction Technology with Emphasis on Two Current Methods for Time Domain Calculation, Journal of Sound and Vibration (1980), 399-419

(19)
Farassat F., Linear Acoustics Formulas for Calculating of Rotating Blade Noise, AIAA Journal, AIAA 80-0996R, VOL. 19, NO.9
(20)
Magliozzi B., Propeller and Propfan Noise, N92-10599
(21)
DFVLR-FAA Propeller Noise Tests In The German-Dutch Wind Tunnel DNW 3, DFVLR-IB 129-86/3
(22)
Succi G.P.: Design of Quiet Efficient Propellers, Transaction of 1979 SAE Business Aircraft Meeting, Paper 790584, April 1979
(23)
Reid, Elliot, G.: The influence of blade-width distribution on propeller characteristics, 1949, NACA Technical Note 1834